ROYAL SOCIETY OF CHEMISTRY

REVIEW

Check for updates

Investigating lithium metal anodes with nonaqueous electrolytes for safe and high-performance batteries

Hui Zhang and Yabing Qi (ID) *

Lithium metal batteries are promising candidates for meeting the increasing demand for next-generation energy storage devices with high energy density; however, the problems of lithium dendrites and unstable solid electrolyte interphases (SEIs) for lithium anodes with nonaqueous electrolytes severely hinder their practical applications. The first step to address these issues is to establish a better understanding about these phenomena. In this review, we first discuss the formation processes and related mechanisms of dendritic lithium and SEIs, which are revealed and supported by the specially designed setups combined with various advanced characterization techniques including *operando* scanning transmission electron microscopy (STEM) and deduced theoretical models. Because of the high sensitivity of lithium metal anodes to the ambient environment, their microscopic characterization remained challenging until the development of noninvasive cryogenic electron microscopy. Then, we present the real-state atomic structures and chemical compositions of lithium dendrites and SEIs by cryogenic transmission electron microscopy (cryo-TEM) coupled with electron energy loss spectroscopy (EELS). Based on these fundamental insights, various strategies including electrolyte engineering, construction of artificial SEI layers, and use of three-dimensional hosts for lithium, introduced to solve the lithium anode problems, are summarized. Finally, the future directions and opportunities regarding lithium anode research are discussed.

1. Introduction

With the ever-increasing demand for advanced energy storage devices with a high energy density (>500 W h kg^{-1}), lithium metal batteries have continued to attract enormous attention because of the relatively high specific capacity (3680 mA h g^{-1}) and low potential (−3.04 V *versus* the standard hydrogen electrode) of lithium metal anodes.[1–6] The first commercial rechargeable lithium metal batteries date back to the 1970s, but these batteries were recalled several years later due to the frequent fire and explosion accidents.[7–9] In traditional lithium metal batteries with liquid nonaqueous electrolytes, lithium dendrites can be readily formed during the charge and discharge cycling, especially when the lithium salt concentration is low or the substrate surfaces are not flat with some protruding points, defects or boundaries[10,11] (Fig. 1). As they grow sharper and longer, the lithium dendrites can penetrate through the polymer separator film, thereby resulting in short-circuits and overheating of low-boiling organic solvents.[12–14] Because the formation of lithium dendrites is largely regulated by the surface properties of the lithium anode, the solid

electrolyte interphases (SEIs) theoretically have the potential to inhibit lithium dendrite formation. However, the naturally formed SEIs on lithium anodes are usually loose and unstable, which cannot restrict lithium dendrite growth because of their inferior mechanical and elastic properties.[15–20] Besides, low-quality SEIs crack and regrow continuously during the repeated lithium plating and stripping, leading to more growth of lithium dendrites and severe waste of lithium metal and electrolyte. Moreover, thick SEIs, "dead lithium" (*e.g.*, broken lithium dendrites from the root and lithium electrically isolated by the surrounding SEIs) and porous lithium can block lithium ion transport, resulting in low capacity, low coulombic efficiency (CE) and poor cycling stability.[21–26]

To revive lithium metal batteries, these two critical problems of lithium dendrites and unstable SEIs related to the safety concerns and cycling stability of batteries need to be solved. Over the past few decades, many attempts have been made to overcome these challenges, including, for example, electrolyte or separator modification and electrode engineering.[27–32] Although the results show that some methods can help improve the battery performance to give higher CE, specific capacity and cycling stability, there is still a long way to go before the practical application of lithium metal batteries can be realized. The most critical reason is the limited in-depth understanding of lithium dendrites and SEIs on lithium anodes until now, which

Energy Materials and Surface Sciences Unit (EMSSU), Okinawa Institute of Science and Technology Graduate University (OIST), 1919-1 Tancha, Onna-son, Okinawa 904-0495, Japan. E-mail: Yabing.Qi@OIST.jp
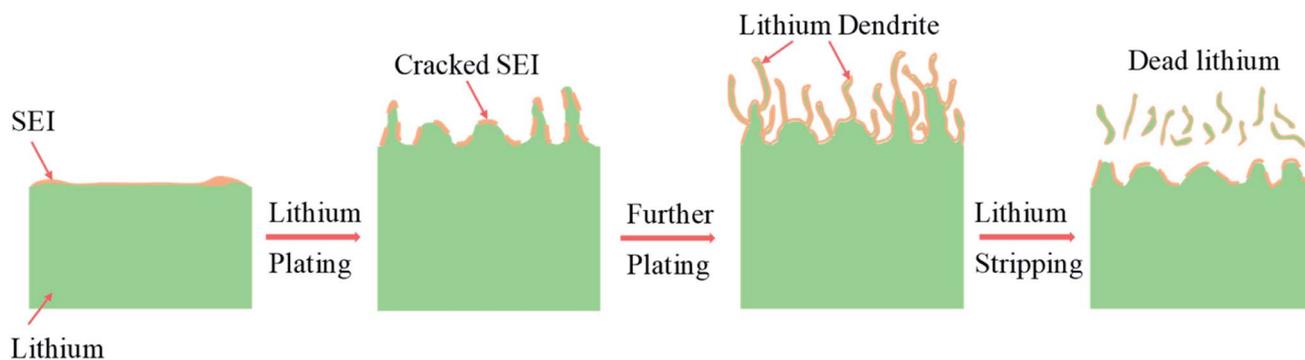
Fig. 1 Schematic drawing illustrating the formation process of SEIs and lithium dendrites during lithium battery cycling.

severely restricts the further development of lithium metal batteries. Various characterization techniques have been employed to reveal the formation processes and structures of lithium dendrites and SEIs, for example, X-ray photoelectron spectroscopy (XPS), scanning electron microscopy (SEM), transmission electron microscopy (TEM) and atomic force microscopy (AFM).[33–36] However, the special treatment before measurement (*e.g.*, washing and drying) and the inherent sensitivity of lithium metal anodes to high energy sources (*e.g.*, electron beams) cast doubt regarding how the obtained results can be correlated with the real state of cycled lithium anodes to provide high-resolution structural or morphological information on lithium anodes. Benefiting from the development of various characterization techniques, *in situ/operando* measurements and characterization of the well-preserved morphology with high resolution have achieved rapid growth in recent years, giving us the opportunity to trace the formation mechanism and obtain atomic morphology information on lithium dendrites and SEIs after repeated cycling, and then explore the corresponding solutions to solve the lithium anode problems.[37–44]

In this review, we examine and provide a concise account of the investigation of lithium metal anodes including the formation mechanisms, chemical and electrochemical properties, morphology, crystal structures and mechanical properties of lithium dendrites and SEIs on them. Furthermore, we have reviewed strategies to inhibit lithium dendrite growth and stabilize the SEI layers. Finally, we provide an outlook to future directions of lithium metal anode research especially regarding the design of high-performance lithium metal batteries with high safety and cycling stability.

2. Formation

In traditional lithium metal batteries with liquid nonaqueous electrolytes, the formation of lithium dendrites and SEIs is considered to occur simultaneously or the latter process occurs earlier than the former one, which still remains controversial.[3,45] Lithium shows high chemical reactivity with almost all nonaqueous electrolytes used in lithium batteries because of its extremely low potential (lower than the reduction potentials of most nonaqueous electrolyte solvents).[11] Previous XPS analyses

of SEIs on lithium metal anodes have demonstrated that after immersing lithium metal in nonaqueous electrolytes for a short period of time (a few minutes), the nonaqueous electrolytes spontaneously decompose to form SEI films on the lithium anode.[45] After loading current, some components of the previously formed SEIs are further reduced to more stable species, and the structures also have corresponding modifications.[45] There are mainly three mechanisms to describe the formation process of SEIs, *i.e.*, the Pedel model, the mosaic model and the coulombic interaction mechanism.[5] In the Pedel model, the chemical interaction between the lithium anode and nonaqueous electrolyte is stepwise and the formed SEIs present an integral structure with point defects for ion migration. In the mosaic model, reduction reactions of all components are considered to take place at the same time and the decomposed multiphase products deposit on the lithium anode in a disorderly manner to form mosaic-type SEIs. As for the coulombic interaction mechanism, reduction products with double electrical layers are stacked layer by layer to generate SEIs with multilayer structures. Although these models based on XPS, FTIR, and electrochemical spectroscopy results and theoretical calculations have enabled researchers to explain the structure of some SEIs, it is desirable to perform in-depth direct investigations on SEIs, which are currently still scarce. Hou *et al.* applied mass-sensitive scanning transmission electron microscopy (STEM) in the low-dose mode to visualize the evolution process of SEIs.[46] As shown in Fig. 2a, a double-layer SEI film is initially formed when the electrolyte is spontaneously decomposed on the electrode surface. The salient contrast difference indicates that the brighter inner layer is composed of compact inorganic compounds (*e.g.*, LiF, Li_2CO_3, Li_2O, *etc.*) and the outer layer mainly contains organic decomposed products with a higher mass density (*e.g.*, ROLi, $ROCO_2Li$, *etc.*, where R stands for the alkyl group). The twisted fine white line is the edge of the SEI (Fig. 2a and b), illustrating the uneven and porous SEI film at the early stage. Electrolytes can permeate through the porous SEI film and contribute to generating a thicker SEI after continuous decomposition reactions (Fig. 2c). Upon further lithiation, the SEI gradually evolves into a thinner, compact and uniform film (Fig. 2d), which is consistent with the activation process in the lithium battery test. Finally, the failure of this SEI is mainly related to the dissolution of the inorganic layer during
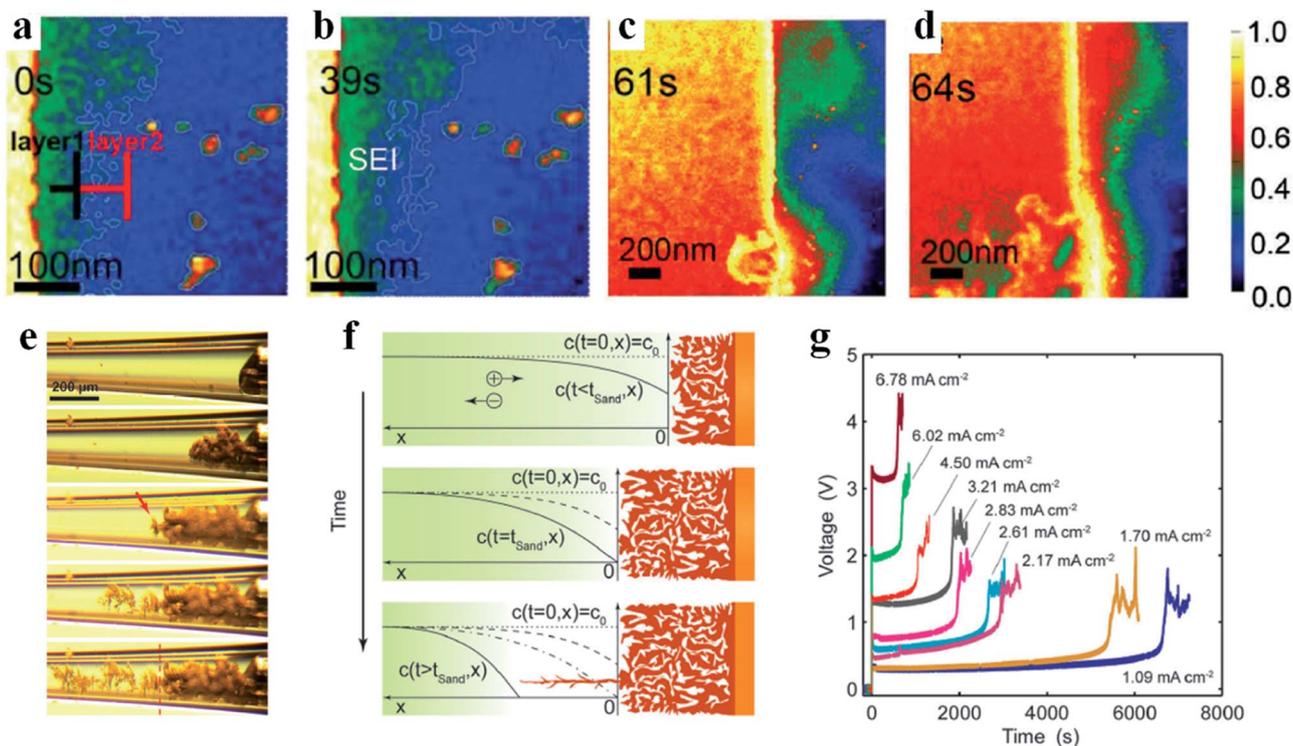
Fig. 2 Formation of SEIs and lithium dendrites. (a–d) Time sequential high-angle annular dark-field STEM (HAADF-STEM) images of SEIs. Reproduced with permission.[46] Copyright 2019, Wiley-VCH. (e) *In situ* optical photograph of lithium growth. (f) Theoretical interpretation of lithium deposition during concentration polarization. (g) Voltage responses under various current densities. Reproduced with permission.[48] Copyright 2016, The Royal Society of Chemistry.

the repeated cycling. However, gold is applied in this experiment instead of lithium metal to act as the electrode, which can only provide some clues for the SEI evolution in lithium batteries. Therefore, the real SEI formation process on the lithium metal anode still awaits exploration. Besides, more models are still needed to explain the increasingly complex SEI phenomena in advanced battery systems (*e.g.*, lithium–sulfur and lithium–air batteries).

After initializing the charging process with current loading, the lithium ions start being electrodeposited on the lithium anode. Because lithium ions exist as solvated forms in the liquid electrolyte, these solvated lithium ions need to shed the solvent molecules first and are then reduced to atoms that are usually adsorbed on the lithium anode surface.[47] The reduced lithium atoms diffuse and incorporate into the underlying metal lattice to complete the nucleation process.[5] However, affected by the rough SEI structures, lithium preferential deposition results in dendritic lithium, which is inclined to crack the fragile SEIs.[9] Reversibly, the broken SEIs provide more nucleation sites for lithium dendrite growth. Therefore, the instability of SEIs is a critical factor for the formation of lithium dendrites. To reveal the lithium dendrite growth mechanism, Bai *et al.* designed a capillary cell to realize the *in situ* observation of the lithiation process.[48] As displayed in Fig. 2e, the initially deposited lithium is present in mossy form, which has no hazardous potential to penetrate through the separator, causing the short circuit problem. After reaching a certain

point, wispy lithium appears and starts to grow into fractal lithium dendrites. These two different deposited lithium forms are distinguished by Sand's time (t_{Sand}), which was proposed by Sand in 1901.[49] At the early electrodeposition stage, the ionic concentration remains steady and therefore lithium ions deposit relatively smoothly from the root to generate mossy lithium, which is a reaction-limited process. When $t = t_{Sand}$, the ion concentration at the electrode decreases to zero, and thus lithium starts to deposit and grow from the tip, leading to the formation of lithium dendrites (Fig. 2f). Different from the reaction-limited mossy lithium, the growth of lithium dendrites is mainly determined by the ion diffusion rate, and therefore it is a diffusion-limited process. In Sand's formula, t_{Sand} is inversely proportional to the current density, meaning that high current promotes the generation of lithium dendrites (Fig. 2g). This is consistent with most reported experimental results.[50,51] However, there are also exceptions when the current density increases beyond a threshold. For instance, in the lithium battery systems proposed by Yan *et al.* and Li *et al.*, the lithium dendrite problem can be alleviated by the self-healing effect of heat treatment and high current density, respectively.[52,53] Combining the experimental and simulation results, the authors have demonstrated that safe-level heating triggered by high current density promotes flux and surface diffusion of lithium, which makes adjacent dendritic particles fuse together and therefore smoothens and stabilizes the dendrite surface.

The cycling stability and CE of lithium batteries are greatly influenced by lithium dendrites and SEIs. Inactive lithium is generally thought to consist of electrochemically formed lithium compounds in the SEI and the electrically isolated lithium metal (*i.e.*, dead lithium), of which the former is assumed to be the main source of capacity loss and low CE. Although there are some assumptions that unreacted lithium also brings about lithium loss and decreases the CE, it is hard to quantitatively distinguish these two lithium sources due to the limited number of efficient characterization techniques. Fang *et al.* designed a delicate titration gas chromatography (TGC) system to quantify the amount of unreacted metallic lithium based on the chemical reaction of $2Li + 2H_2O = 2LiOH + H_2\uparrow$.[54] In this TGC system, the reacted lithium anode is first transferred to a sealed container. After the reaction with H_2O added by gas-tight syringe, the formed H_2 is measured by gas chromatography, and thus the amount of unreacted metallic lithium can be calculated accordingly. The TGC results demonstrate that it is the unreacted metallic metal other than lithium compounds that dominates the capacity loss. However, the formation of inactive lithium is intimately correlated with the SEIs. Therefore, to explore advanced strategies to improve the electrochemical performance of lithium metal batteries, the two aspects of lithium dendrites and SEIs are regarded as a whole part for studies in the following sections.

3. Morphology and surface chemistry

It is difficult to characterize the morphology of lithium dendrites and SEIs with high resolution by common characterization techniques. The major reasons are the unique structural and chemical properties of lithium metal anodes including nanoscale morphology, multicomponent chemical composition, reactivity with oxygen and moisture and high sensitivity to the atmosphere and high-energy sources, such as electron beams. Established morphological characterization techniques such as optical microscopy and scanning probe microscopy (*e.g.*, AFM) are commonly used to minimize the sample damage induced by the characterization process.[55–57] However, the low-resolution results and special electrode setup make it difficult to achieve high-magnification structural identification and reveal the real situation of lithium dendrites and SEIs in lithium metal batteries, respectively. The lithium anode is cycled and evolves in liquid nonaqueous electrolyte, so its real morphological and structural measurements should take the liquid state into account, which is nonetheless challenging for most characterization techniques.

Inspired by the application of cryogenic techniques in biology, Zachman *et al.* froze the sample first using a cryogen to preserve the initial structure of the lithium anode.[58] Then, combining the cryo-focused ion beam (cryo-FIB) and analytical cryo-STEM, relatively high-resolution cross-sectional images of the cycled lithium anode were obtained. As shown in Fig. 3a, two different types (Types I and II) of lithium dendrites appear at the same time after being cycled in commercial carbonate electrolyte, which is different from the previous reports with only one type (whisker-like or rod-like) of lithium dendrite in one battery system (Fig. 2b and c).[54,59] The difference may be caused by the washing and drying operations in traditional sample preparation, which change the original structure of the cycled lithium anode to some extent. The Type I dendrite presents an irregular ellipse-like shape and the average size is about 5 μm (which can be classified into mossy lithium), while the Type II lithium dendrite is more like a long (about 10 μm) branch (*i.e.*, dendritic lithium) with a length of hundreds of nanometers (Fig. 3a). Furthermore, more information about the spatial distribution of these dendrites is provided by the reconstructed three-dimensional (3D) structures of these two different dendrites based on the consecutive cross-sectional images (Fig. 3d). An interesting phenomenon here is that these two types of dendrite show a similar number of occurrences, implying that there is no preferred growth for any kind of dendrite, which is correlated with their formation mechanism. The main constituents of Type I and II dendrites are partially oxidized lithium and LiH, respectively. LiH forms from the reaction between the deposited lithium and organic electrolyte. Because almost all organic electrolytes contain hydrogen, there is a high chance to generate Type II lithium dendrites during the charge and discharge process. However, Type II dendrites can easily lead to low CE and high capacity fading rate for the following reasons: (1) LiH is fragile, (2) LiH has low conductivity, and (3) Type II dendrites have limited contact area with the current collector, all of which result in a high portion of "dead lithium". Except the inactive lithium and lithium dendrites, the pulverization of the lithium anode is another severe factor that leads to its failure during the repeated charge and discharge process. However, the origin of the pulverization remains controversial. L. F. Kourkoutis identified dendritic LiH in the pulverized lithium anode, which might result in capacity fading.[58] Nevertheless, no LiH is detected in the studies by Yi Cui *et al.* and Y. S. Meng *et al.*[54,59] Considering the situation that the results from Yi Cui *et al.* and Y. S. Meng *et al.* are based on the Li/Cu half cells, G. Xu *et al.* adopted the practical $Li/LiCoO_2$ batteries to unravel the presence of LiH.[60] Through the on-line gas analysis mass spectrometry system with a differential electrochemical mass spectrometry system and D_2O titration gas analysis mass spectrometry system, LiH is confirmed to be the dominant species related to the lithium pulverization. The continuous electrolyte and electrode parasitic reactions give rise to the formation of H_2, which can actively react with lithium to generate LiH. To regulate the lithium growth, Z. Ju *et al.* applied a biomacromolecular matrix from the inner film of the eggshell as the medium to suppress lithium dendrites.[61] Specifically, this biomacromolecular matrix is a trifluoroethanol-modified eggshell membrane. It possesses a three-dimensional porous structure with a thickness of about 90 μm, which is composed of cross-linked protein fibers. The main elements of the modified eggshell membrane are C, N, O, S and F. As shown in Fig. 3e, a lithium sphere was deposited and grew preferentially along the ⟨110⟩ direction after the
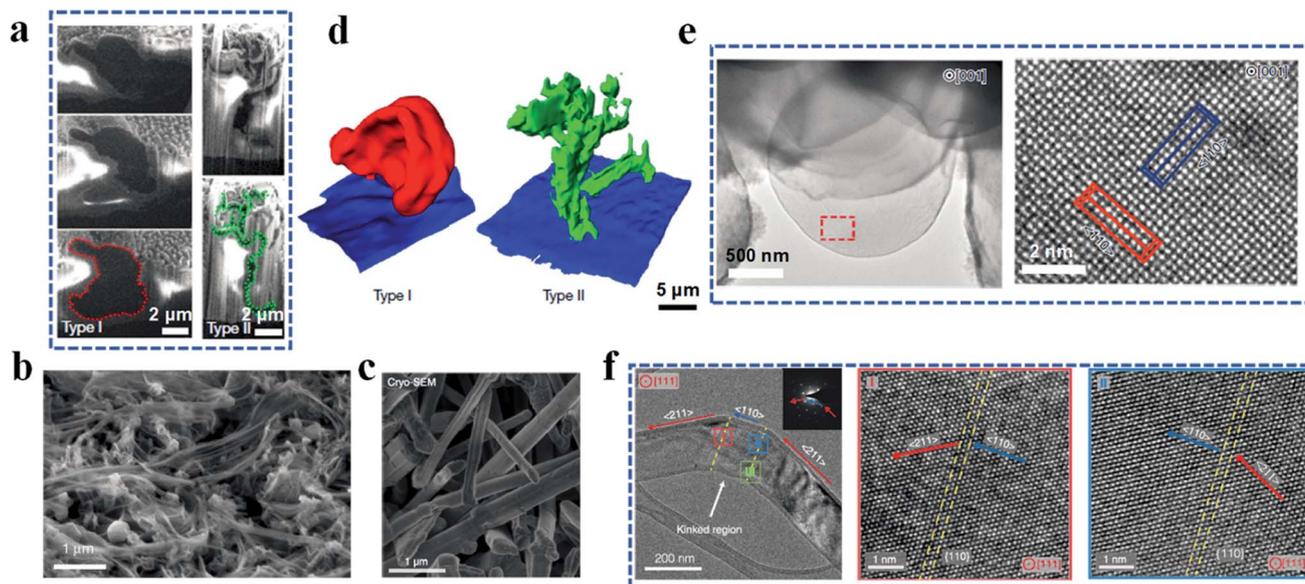
Fig. 3 Lithium dendrite characterization by cryogenic techniques. (a) Two distinct dendrites referred to as Types I and II by cryo-FIB and cryo-SEM. Reproduced with permission.[58] Copyright 2018, Springer Nature Ltd. (b) Whisker-like lithium cryo-SEM image. Reproduced with permission.[54] Copyright 2019, Springer Nature Ltd. (c) Rod-like lithium cryo-SEM image. Reproduced with permission.[59] Copyright 2017, American Association for the Advancement of Science. (d) Reconstructed 3D structures of lithium dendrites. (e) Cryo-TEM images of a lithium microsphere and its corresponding atomic structure. Reproduced with permission.[61] Copyright 2020, Springer Nature Ltd. (f) Atomic structure of a lithium dendrite obtained by cryo-TEM. Reproduced with permission.[59] Copyright 2017, American Association for the Advancement of Science.
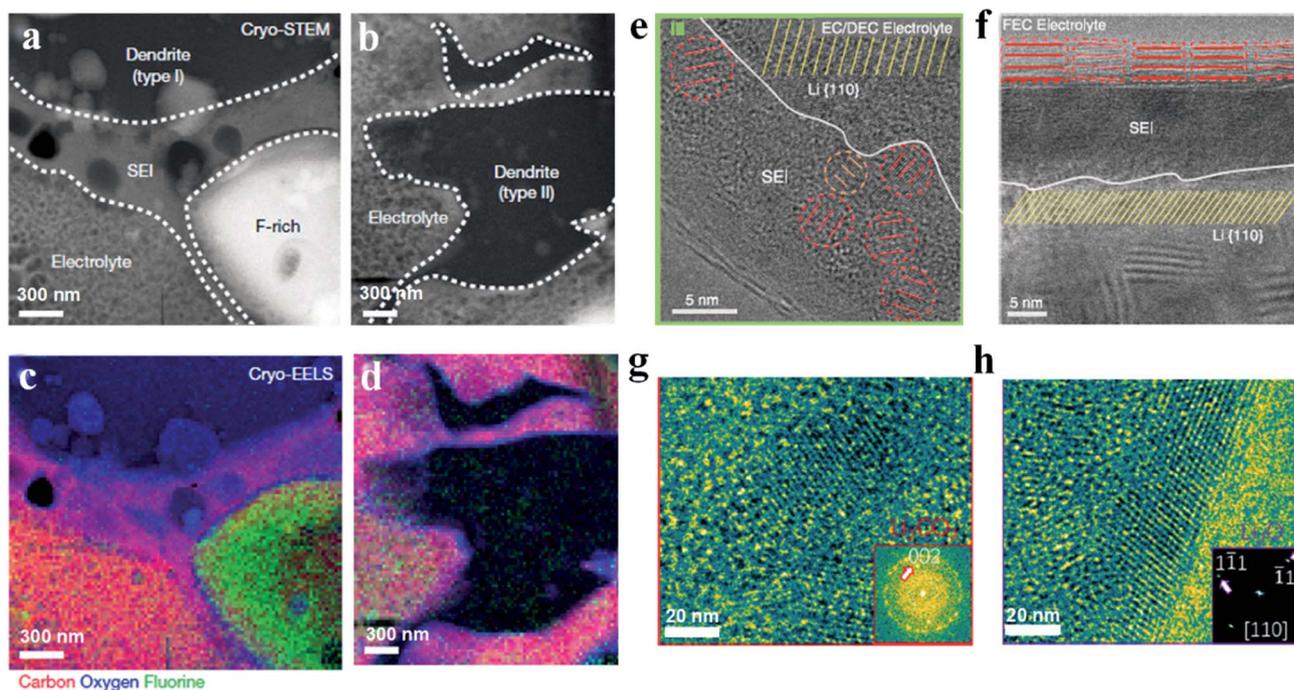
Fig. 4 Characterization of SEIs by cryogenic techniques. (a–d) Cryo-STEM images (a and b) and corresponding cryogenic electron energy loss spectroscopy (cryo-EELS) mapping (c and d) of two lithium dendrites and SEIs. Reproduced with permission.[58] Copyright 2018, Springer Nature Ltd. (e) Mosaic SEI atomic structure and (f) atomic structure of multilayer SEIs. Reproduced with permission.[59] Copyright 2017, American Association for the Advancement of Science. (g and h) Atomic mosaic structure of the SEI in the vinylene carbonate-treated lithium deposition system. Reproduced with permission.[62] Copyright 2020, American Chemical Society.

biomacromolecular treatment. In contrast, dendritic lithium was observed on the pure lithium metal surface, and the atomic structures from cryo-TEM show that lithium dendrites grow along two different directions, ⟨110⟩ and ⟨211⟩, and the growth direction can be changed from ⟨110⟩ to ⟨211⟩ in the kinked regions (Fig. 3f).

Coupled with cryo-TEM, electron energy loss spectroscopy (EELS) with better resolution for light elements than energy dispersive spectroscopy (EDS) works under cryogenic conditions to reveal the chemical compositions and distributions of SEIs. As shown in Fig. 4, influenced by the difference of lithium dendrites, SEIs also show various morphologies. Specifically, SEIs around Type I dendrites are about 300 to 500 nm thick, and are mainly composed of lithium ethylene dicarbonate with bubbles from ethylene gas, which is a kind of by-product from ethylene carbonate during the production of lithium ethylene dicarbonate (Fig. 4a). Besides, there is a large fluorine-rich structure up to micrometers in size around Type I dendrites and it is surrounded by SEIs. However, Type II SEIs are compact and thin (approximately 20 nm thick) with Li_2O and $LiOH \cdot H_2O$ as the main components (Fig. 4b). Besides lithium dendrites, SEIs are also largely influenced by electrolyte compositions, because SEIs are essentially decomposed products of electrolytes. In commercial carbonate electrolytes with fluorine-containing salts, SEIs mainly contain Li_2CO_3, Li_2O and LiF, and present as "mosaic SEIs". As shown in Fig. 4e, Li_2CO_3 and Li_2O crystalline nanoparticles are dispersed in an organic polymer matrix. However, after adding a small amount of fluoroethylene carbonate (FEC), which is a common electrolyte additive to improve the performance of lithium metal batteries, "multilayer SEIs" appear. The inner layer is a polymer matrix and the outer one is composed of large Li_2O grains with clear lattice fringes (Fig. 4f). Different from FEC, vinylene carbonate (another common additive to achieve high CE for lithium batteries) promotes the formation of mosaic-like SEIs with Li_2CO_3 and Li_2O nanoparticles after slight oxidation with lithium metal (Fig. 4g and h).[62] Although carbonate-based electrolytes are commonly used in lithium batteries, SEIs formed from them are always thick, unstable and fragile, leading to low CE and fast capacity fading. As an alternative, ether-based electrolytes are introduced and widely used in lithium–sulfur and lithium–oxygen batteries, because they always show high efficiency (>98%) and efficient dendrite suppression. On the basis of the XPS and SIMS analyses, it has been demonstrated that except the inorganic components (e.g., Li_2CO_3, Li_2O, LiOH, LiF, etc.) and organic species (e.g., RCOOLi and RCH_2OLi), oligomers are also formed in some ether-based electrolytes, which show high flexibility and good conformity with the lithium metal to accommodate the lithium volume variations and suppress lithium dendrites during the continuous plating and stripping process.[11,45] The chemical properties and structures of SEIs are determined by the electrolytes including the concentration, salts and solvents, which provide a valuable opportunity to modify SEIs and therefore improve the lithium battery performance.

4. Strategies to improve the lithium metal anode

As summarized above, lithium dendrites and low-quality SEIs are two main problems causing the low CE, heat throwaway, and severe side reactions at the side of lithium anodes. Based on the fundamental understanding, a lot of efforts have been made to block lithium dendrite growth by physical shielding or regulating the lithium ion flux. Generally, there are four typical ways to solve these problems and improve the lithium metal battery performance: (1) electrolyte engineering, (2) constructing artificial SEI layers and (3) a three-dimensional (3D) lithium framework, and (4) using solid state electrolytes. As the lithium dendrites and SEIs are intimately correlated, all these mentioned strategies have the potential to simultaneously address these two issues of lithium anodes.

4.1. Electrolyte engineering

As discussed before, the components of the liquid nonaqueous electrolyte play an important role in regulating the lithium deposition and SEI formation, and therefore various kinds of electrolyte system have been reported to suppress lithium dendrites and stabilize the SEI layers, which can be classified into (1) additive-assisted electrolytes, (2) high concentration electrolytes (HCEs), (3) localized high concentration electrolytes (LHCEs) and (4) liquefied gas electrolytes proposed recently by Meng et al. exhibiting excellent performance under low-temperature working conditions.

Halogen containing compounds are commonly used additives in carbonate electrolytes, such as hydrofluoric acid (HF), fluoroethylene carbonate (FEC), vinylene carbonate (VC), silicon tetrachloride $(SiCl_4)$, thionyl chloride $(SOCl_2)$, tris(2,2,2-trifluoroethyl) borate (TTFEB) and $CsPF_6$.[63–70] One common feature of these various additives is that they can form lithium halides (LiF or LiCl) within the SEI layers through chemical reactions with lithium metal, and previous reports have demonstrated that high lithium halide content is thermally favorable for the reactions in SEIs, inducing uniform lithium deposition.[71] In addition, introduction of halogen-free compounds into the electrolyte can also produce lithium halides, improve SEI quality and therefore alleviate the lithium dendrite problem. For example, Qian et al. reported that a trace amount of water leads to the decomposition of $LiPF_6$ to HF, which further reacts with lithium metal to form LiF-rich SEI layers.[72] However, these functionalized SEIs strongly depend on the amount of additives in the electrolyte, so if the additives are consumed during the long-term cycling process, lithium dendrites and unstable SEIs will reappear. To address this challenge, Wang et al. introduced a small amount of lithium iodide (LiI) into an ether-based electrolyte to induce organic solvent polymerization, in situ forming flexible oligomers within SEIs.[73] Therefore, the obtained SEI layers possess both high elasticity and excellent ionic conductivity, which not only suppress lithium dendrites, but also promote lithium ion transport. More importantly, this electrolyte has the potential to be applied in long lifespan

lithium batteries because of the low reliance on additive concentrations.

Because most undesired organic components (*e.g.*, ROCOOLi and RCOOLi) in SEI layers originate from organic solvents, increasing the salt concentration to produce more inorganic products within SEIs becomes an effective way to achieve thin, dense and highly ion-conductive SEI layers.[74] Fan *et al.* reported a high concentration electrolyte with 10 M lithium bis(fluorosulfonyl)imide (LiFSI) dissolved in a binary solvent of ethylene carbonate (EC) and dimethyl carbonate (DMC) applied in lithium metal batteries to construct high-quality SEIs (Fig. 5). Compared with the diluent electrolyte (1 M LiFSI), SEIs from the high concentration electrolyte show a higher F and S content but a lower C and O content, which indicates that the high concentration of LiFSI contributes to more LiF formation but less adverse organic species (Fig. 5a and

b). LiF has been verified to play critical roles in blocking the side reactions and promoting lithium ion transport; therefore, the deposited lithium in high concentration electrolyte displays a round-shape morphology. However, dendritic lithium appears in dilute electrolyte (Fig. 5c and d). Furthermore, through AFM measurements, Wang *et al.* demonstrated that high concentration LiFSI helps to create high-modulus SEIs, which act as strong physical shields to further suppress lithium dendrites.[75] Therefore, similar to other additives in an electrolyte, the role of high concentration electrolyte is to modify the SEI structure and promote the generation of favorable inorganic salts (*e.g.*, LiF).

Despite the ability to fabricate high-quality SEI layers, high concentration electrolytes have limitations in practical applications, for example, poor ionic conductivity, poor wetting capability and high viscosity.[76,77] In recent years, localized high concentration electrolytes applying diluent to dilute high concentration
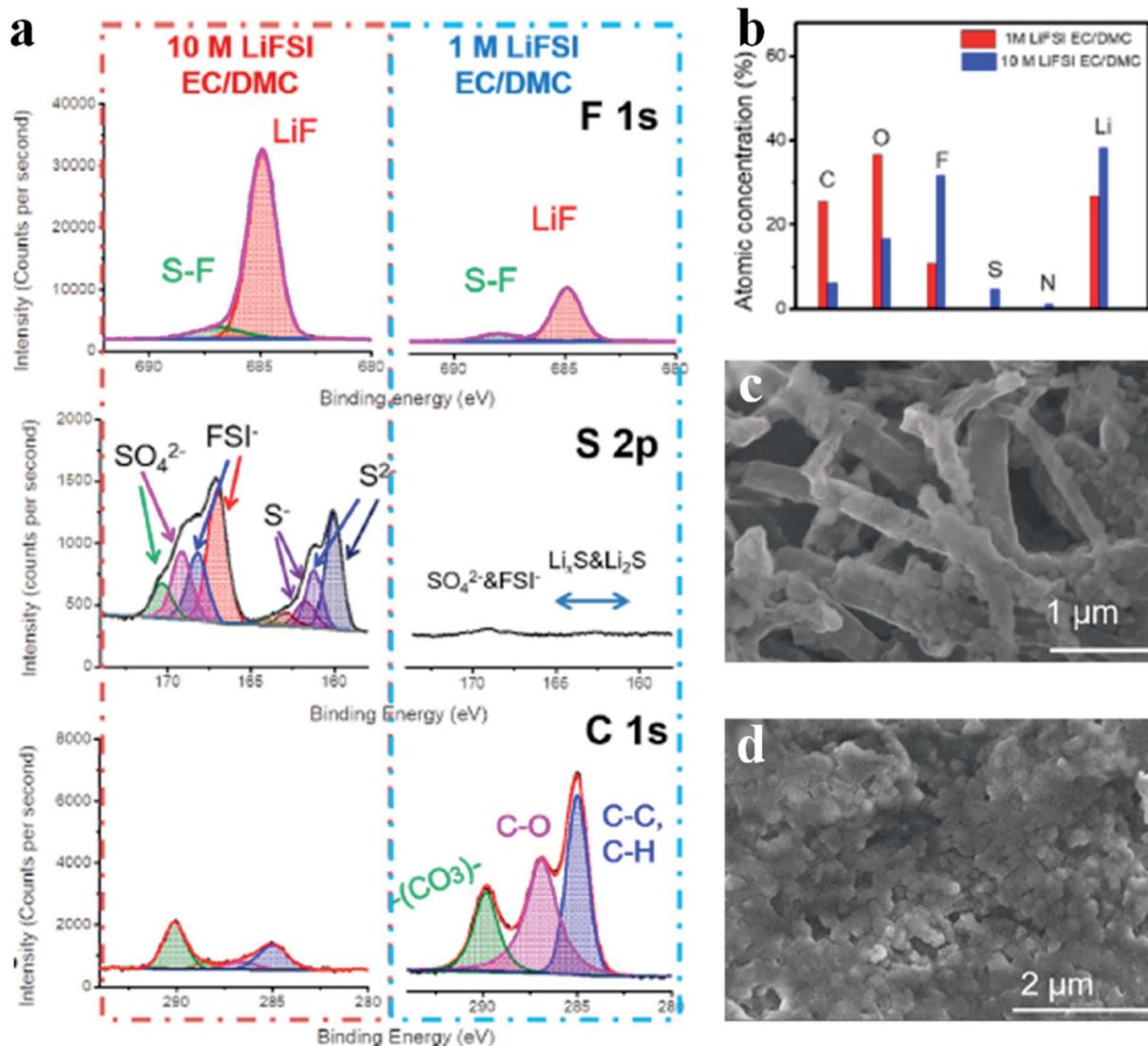
Fig. 5 High concentration electrolyte strategy to improve lithium anodes. (a) XPS profiles for SEIs of lithium metal cycled in concentrated and dilute electrolytes; (b) elemental concentrations obtained from the XPS results; (c and d) surface morphologies of the lithium anode cycled in concentrated (c) and dilute electrolytes (d). Reproduced with permission.[74] Copyright 2018, Elsevier Inc.

electrolytes have attracted intense research interest.[78–81] In this system, the diluent is inert enough to dissolve the salts but miscible with the solvent; therefore the solvation structure of the high concentration electrolyte is preserved well, while the salt concentration and viscosity are lowered to a practical level. For example, Ren et al. introduced a non-solvating fluorinated ether of 1,1,2,2-tetrafluoroethyl-2,2,3,3-tetrafluoropropyl ether (TTE) to dilute highly viscous tetramethylene sulfone.[78] In this sulfone-based localized high concentration electrolyte system, not only have the viscosity and separator wettability been improved (Fig. 6a), but the side reactions at the lithium anode have also been greatly suppressed, and therefore, the resulting SEI layers are flat and thin. Furthermore, fewer carbides and a higher concentration of LiF and Li_xN were detected by depth profiling XPS in high concentration electrolyte and localized high concentration

electrolyte, when compared with diluent electrolyte. It is demonstrated that the diluent can retain its unique properties to create highly ion conductive and uniform SEIs while circumventing the limitations of high concentration electrolyte (Fig. 6b–d).

Nonetheless, the low temperature working ability and inferior rate capability are big challenges that hinder the practical application of localized high concentration electrolyte. Recently, a liquefied gas electrolyte has been developed, which possesses excellent stability with lithium anodes and low viscosity to facilitate lithium ion transport at low temperature.[82,83] In a liquefied gas electrolyte study by Yang et al., a high pressure-liquefied mixture of fluoromethane and carbon dioxide acts as the solvent. LiTFSI and tetrahydrofuran (THF) are the salt and cosolvent, respectively. Because of the high stability with lithium anodes, lithium deposition induced by the
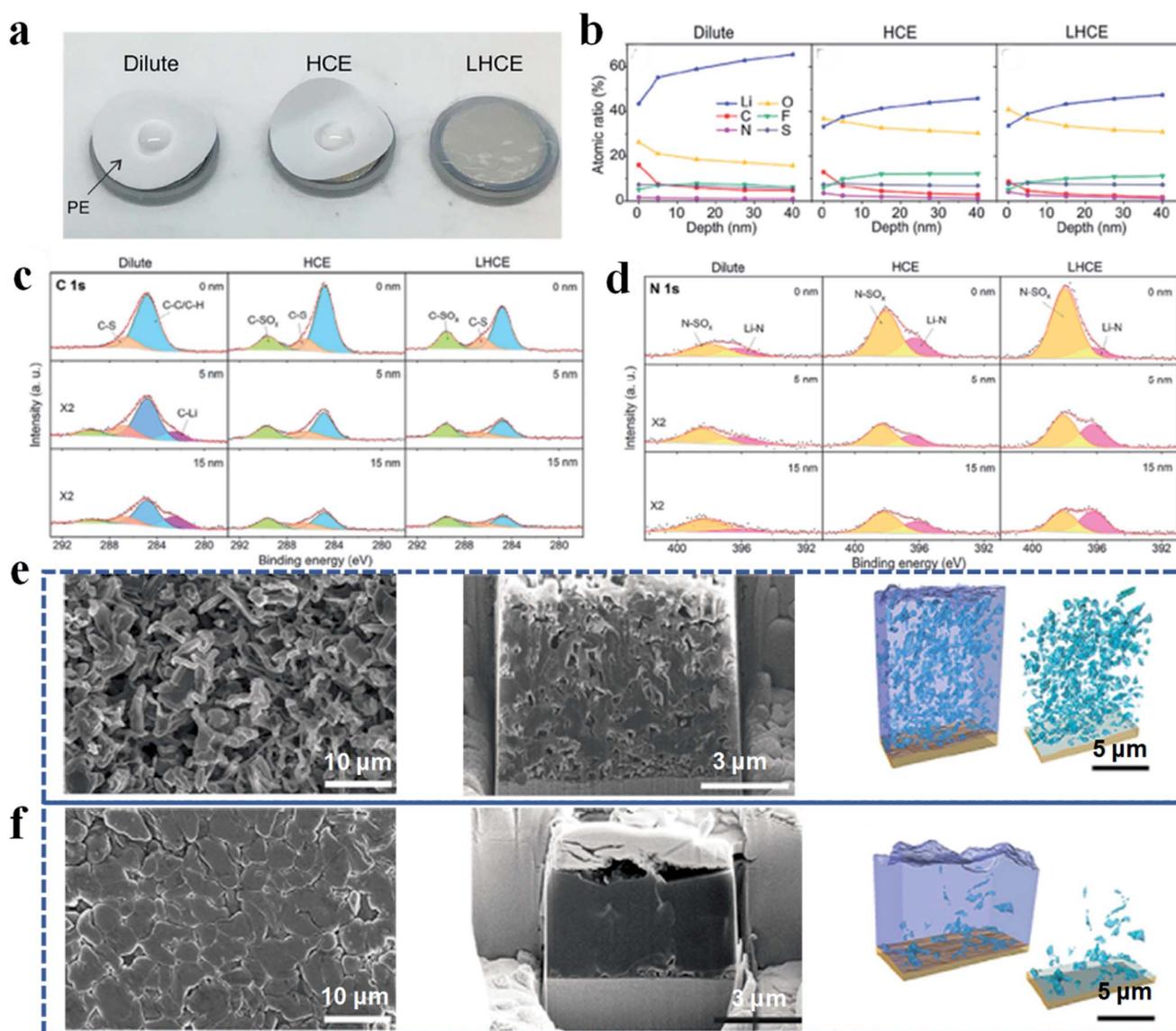
Fig. 6 Application of localized high concentration electrolyte and liquefied gas electrolyte in improving the lithium anode. (a) Wettability test of electrolytes to the separator; (b–d) XPS depth-profiling analysis of SEIs. Reproduced with permission.[78] Copyright 2018, Elsevier Inc. (e and f) Cryo-FIB characterization and 3D construction of a cycled lithium anode in traditional carbonate electrolyte (e) and liquefied gas electrolyte (f). Reproduced with permission.[83] Copyright 2019, Elsevier Inc.

liquefied gas electrolyte is denser and much more uniform than that in conventional carbonate-based electrolyte (Fig. 5e and f). Besides, the electrochemical performance of liquefied gas electrolyte-based lithium batteries is well maintained at low temperature (down to −60 °C) owing to the low melting point and low viscosity of the electrolyte, therefore improving the electrolytic conductivity and low interfacial resistance of lithium batteries.

4.2. Artificial SEI layers

The natural SEIs formed from the reactions between the lithium metal anode and liquid electrolyte are always fragile, loose and thick, and thus not only block ion transport, but also exacerbate the lithium dendrite growth. Therefore, a lot of efforts have been devoted to construct artificial SEIs with excellent robustness and ionic conductivity on a lithium anode to accommodate the infinite volume variations of lithium metal, suppress lithium dendrites and promote lithium ion transport.[84]

According to the chosen materials, artificial SEI layers can be divided into two categories: inorganic and organic SEIs.[84] Inorganic artificial SEI layers such as metal oxides (Al_2O_3 and Li_3PO_4), sulfides, and LiPON have been proven to have remarkable mechanical properties, good electrochemical stability over a wide potential window, and efficient lithium ion transport pathways, but the intrinsic brittleness and inferior conformity with the lithium metal make inorganic artificial SEI layers crack easily during the continuous charge and discharge process, resulting finally in the failure of lithium metal batteries.[85–88] As for the organic SEI layers, although polymer-based products show a poor mechanical modulus and relatively low ionic conductivity, their excellent flexibility and processability effectively modulate lithium ion diffusion, restrict lithium dendrite growth and therefore improve the electrochemical performance of lithium metal batteries.[89]

In order to combine the advantages of both inorganic and organic artificial SEI layers, efforts to fabricate inorganic and organic hybrid artificial SEI layers have received more and more attention recently.[90] For example, Gao et al. developed polymer–inorganic SEIs based on poly(vinylsulfonyl fluoride-ran-2-vinyl-1,3-dioxolane) (P(SF-DOL)) lithium salts embedded with LiF nanoparticles and graphene oxide (GO) nanosheets, in which the dense polymer–nanoparticle part provides effective passivation, and GO nanosheets serve as the mechanical support because of their superior tenacity and mechanical strength. Different from the spontaneously formed SEIs, the components of these hybrid artificial SEIs mainly contain –SO_2–Li, –C–O–Li and LiF from the high resolution XPS results (Fig. 7a). From the SEM and optical profilometry results, the artificial SEIs effectively suppress lithium dendrites and maintain a flat surface after long-term cycling (Fig. 7b–d). In addition, because of the excellent ionic conductivity and liquid electrolyte swelling behavior, this kind of hybrid artificial SEI layer efficiently improves the battery performance under lean electrolyte conditions. Furthermore, the advantageous on-site formation process endows the SEI layers with good homogeneity.

Because of the better conformity with the lithium metal anode and a relatively simple fabrication process, in situ SEI formation is another hot research direction in the field of artificial SEI layers.[91]
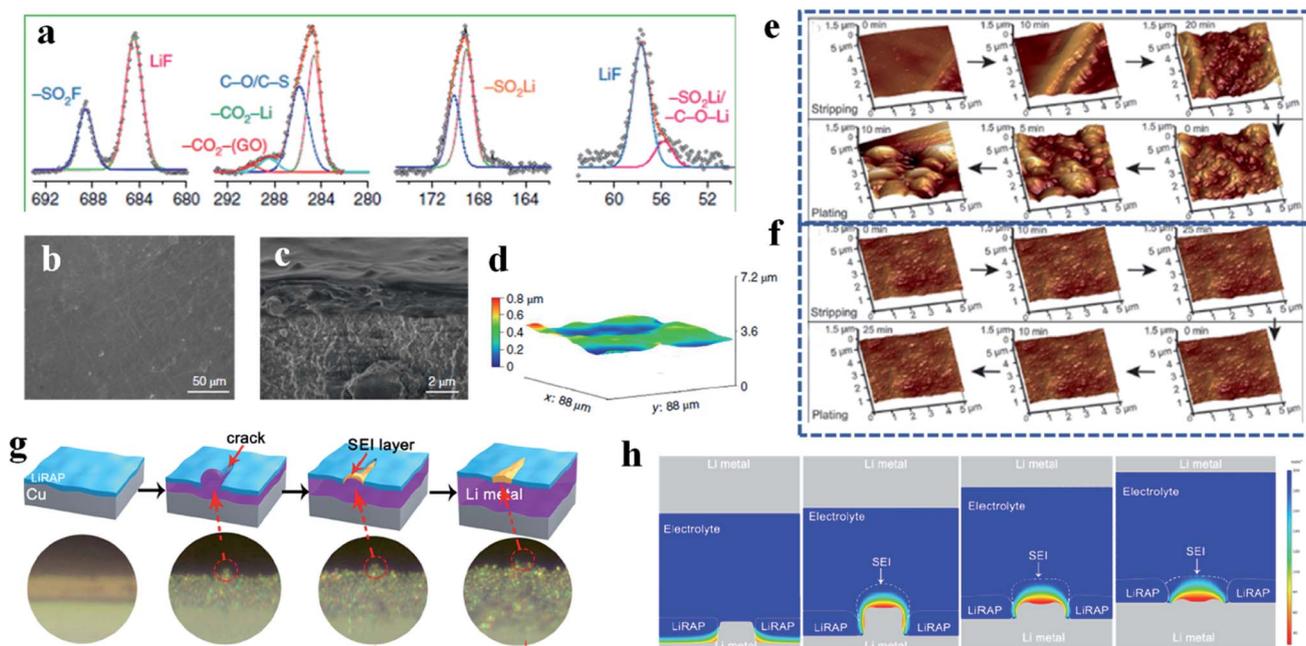
Fig. 7 Artificial SEIs. (a–d) High-resolution XPS spectra (a), SEM pictures (b and c) and optical profilometry image (d) of the hybrid artificial SEI layer. Reproduced with permission.[90] Copyright 2019, Springer Nature Ltd. (e and f) In situ AFM characterization of pristine lithium (e) and LiPPA–lithium (f) during the plating and stripping process. Reproduced with permission.[92] Copyright 2018, Wiley-VCH. (g) Schematic and operando optical microscopy images of the self-regulated lithium metal growth process; (h) COMSOL Multiphysics simulation of the lithium metal deposition process. Reproduced with permission.[93] Copyright 2020, American Chemical Society.

Li *et al.* fabricated a lithium polyacrylic acid (LiPPA) SEI layer by an *in situ* method.[92] Furthermore, with the help of the *in situ* AFM characterization technique, it can be clearly detected that a lot of dendritic structures are generated on the pristine lithium plate during the plating and stripping process (Fig. 7e). In contrast, after being coated with LiPPA, the lithium anode surface remains flat and uniform during the whole working process (Fig. 7f), which proves that the *in situ* formed polymer film is robust enough to suppress the lithium dendrite growth.

Although the goal of introducing artificial SEI layers with relatively high mechanical strength is to resist rupture by the lithium dendrites, some artificial SEIs are likely to be damaged in practical applications, especially inorganic artificial SEIs after long-term cycling.[93] Recently, Han *et al.* reported a special kind of artificial SEI based on lithium-rich anti-perovskites, which has self-regulating capability. Through characterization by *operando* optical microscopy, the self-regulated process is vividly monitored (Fig. 7g). Specifically, different from the traditional SEIs formed from the reduction reaction between lithium metal and liquid nonaqueous electrolyte, these self-regulated artificial SEIs interact with the protruding lithium dendrite after being cracked to form a SEI-like structure, which acts as an adhesive to bind the spliced artificial SEIs and suppress the further growth of lithium dendrites. With the help of COMSOL Multiphysics simulation, it is verified that the newly formed SEI-like structure after self-healing can efficiently regulate the lithium ion diffusion and therefore solve the lithium dendrite problem, improving the cycling stability of lithium metal batteries (Fig. 7h).

4.3. 3D framework hosts

Although the methods of electrolyte engineering and construction of artificial SEI layers have shown great promise to regulate lithium plating and stripping, construct stable SEIs and suppress lithium dendrites, the infinite volumetric variation of lithium metal during the working process because of its intrinsic "hostless" feature is still a huge challenge. Therefore, various 3D framework hosts have been proposed and widely studied in recent years. Furthermore, introduction of a 3D host framework can decrease the effective current density and regulate the lithium flux.[94–96]

Because of the cost effectiveness and good conductivity, various metal-based 3D frameworks with different porosities and modifications are used as porous current collectors for lithium anodes. For example, the nickel foam reported by Chi *et al.* was directly put on molten lithium to fabricate a Li–Ni composite, in which all the large pores of the nickel foam were filled with molten lithium, and the composite surface was relatively smooth (Fig. 8).[97] Owing to the four advantages of nickel foam, *i.e.*, (1) low surface energy to facilitate lithium infusion, (2) high thermal stability to withstand the high temperature during the lithium infusion process, (3) high porosity to accommodate sufficient lithium metal and (4) interconnected electronic and ionic pathways to promote fast electron and ion transport, lithium dendrites are efficiently inhibited and the full cells based on the Li–Ni anode show improved rate capability, low polarization and reduced internal resistance (Fig. 8a–c). It has been demonstrated that the pore structure (*e.g.*, pore size and distribution of the pores) of the metal-based framework has a strong influence on the capability of the hosts to regulate lithium deposition and SEI formation; however, it is not possible for most metal-based 3D frameworks to precisely control the pore structures because of the complex processes. Zhao *et al.* therefore developed an electrochemical etching method to prepare 3D compact copper with uniform porous structures.[98] The obtained uniform and smooth porous copper network helps to form a stable SEI layer and regulate smooth lithium plating and stripping to inhibit lithium dendrite growth. Therefore, the full cells paired with LiFePO$_4$ show enhanced rate performance and cycling stability. However, a big problem of the metal-based framework is the high weight of metal materials, which significantly decreases the energy density of lithium batteries.

Compared to metal-based 3D frameworks, carbon-based frameworks not only have the advantage of being lightweight but also possess high surface area with porous structures, especially for nanocarbon materials including carbon nanotubes (CNTs) and graphene. For example, Sun *et al.* applied a robust CNT paper as a freestanding host to accommodate lithium deposition.[99] Because of the excellent flexibility and mechanical properties, the CNT paper efficiently inhibits the growth of lithium dendrites and withstands the volume change of lithium during the continuous charge and discharge process. It is interesting to note that the deposited lithium on the CNT surface cannot be completely peeled off after the stripping operation, and thus the CNT framework with the lithium residue can act as a pre-lithiated host for future use. Inspired by this idea, Yang *et al.* utilized the pre-lithiation behavior of the CNT sponge to improve the affinity of the host framework with the deposited lithium.[100] Besides, the highly porous CNT sponge provides a high density of lithium nucleation sites and promotes uniform lithium deposition. As a result, dendrite-free lithium plating is realized with the support of the porous CNT sponge with "pre-lithiation" behavior.

Another critical factor that influences lithium nucleation and growth is the affinity of lithium metal to the substrate surface, which is also called lithiophilicity. Previous research has demonstrated that the lithiophilic surface is correlated with the lower plating overpotential of lithium metal compared with the lithiophobic surface, which favors lithium wetting on the substrate and uniform growth.[101] Unfortunately, pristine carbon host materials and the most commonly used copper networks are usually lithiophobic. Therefore, Huang *et al.* developed 3D nanoporous nitrogen-doped graphene to improve the lithiophilic properties of the graphene framework.[102] Owing to the properties of high surface area, good electrical conductivity and excellent affinity to lithium deposition, dendrite-free lithium plating and stripping are guaranteed, and furthermore, the large volume variations of lithium metal during the battery working process are efficiently accommodated (Fig. 8d). As for the copper host, Zhai *et al.* reported a hybrid structure of artificial SEIs on the 3D copper network to promote uniform lithium deposition and therefore improve the lithium anode
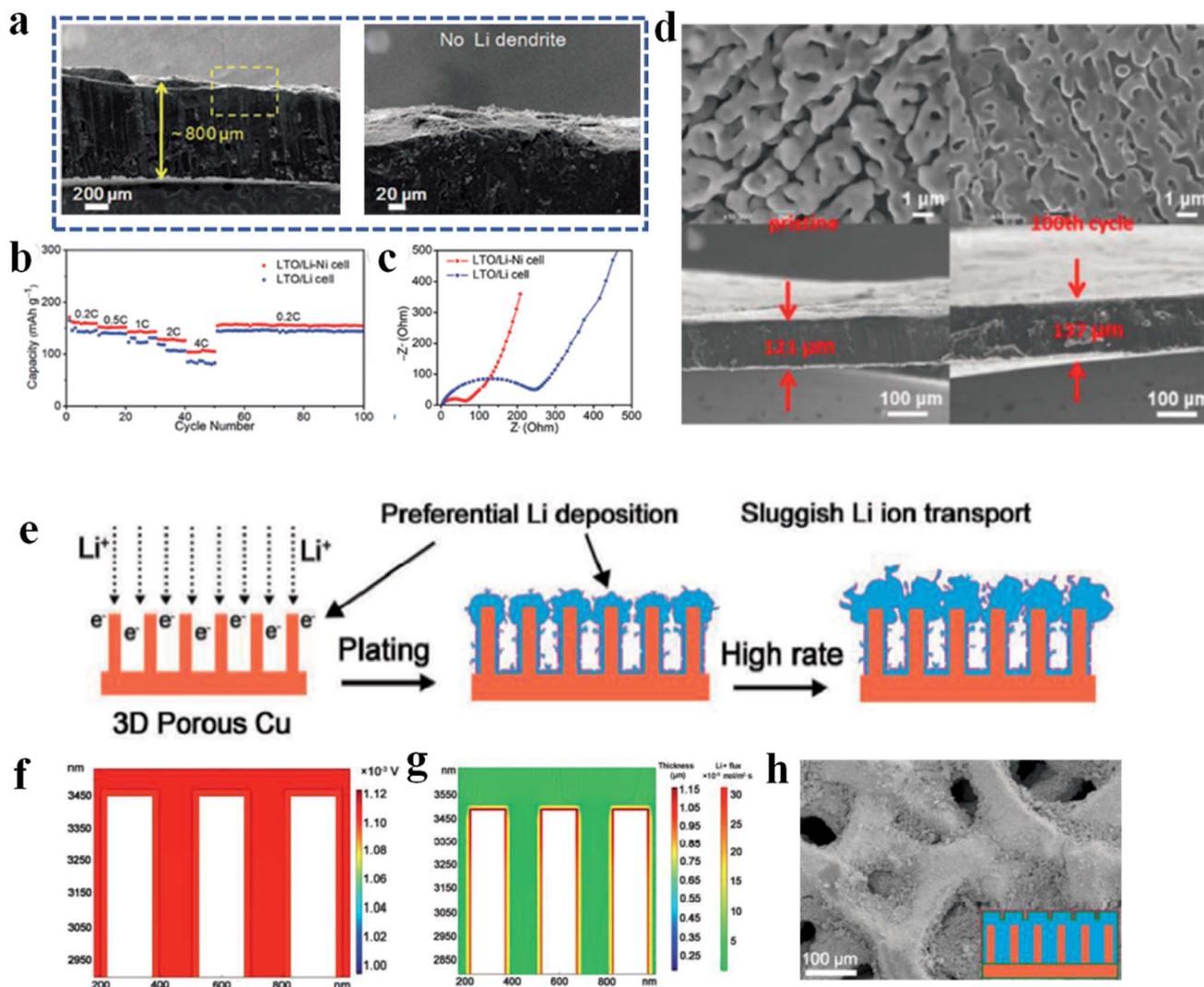
Fig. 8   3D host framework. (a) Cross-sectional SEM images of the cycled Li−Ni anode; (b) rate capability of full cells paired with $Li_4Ti_5O_{12}$ (LTO); (c) resistance measurement of full cells after 100 cycles. Reproduced with permission.[97] Copyright 2017, Wiley-VCH. (d) SEM images of 3D nanoporous nitrogen-doped graphene before and after lithium plating. Reproduced with permission.[101] Copyright 2019, Wiley-VCH. (e) Schematic of lithium deposition behavior on 3D porous copper; (f and g), COMSOL Multiphysics simulations of potential distribution (f) and lithium flux (g); (h) SEM image of the hybrid 3D host framework after continuous lithium plating. Reproduced with permission.[102] Copyright 2020, Wiley-VCH.

performance at a high current density.[103] As shown in Fig. 8e, the naturally formed unstable SEIs on 3D porous copper result in sluggish lithium ion transport and preferential lithium deposition, especially at a high charge and discharge rate, and therefore, it is necessary to further construct stable SEIs on a 3D current collector. In this report, Cu_2S nanowires were grown on the copper skeleton and utilized as the artificial SEIs. Benefiting from the compositional uniformity and high lithium ion conductivity, the hybrid 3D host framework with artificial SEIs facilitates rapid lithium ion transport, uniform potential distribution and flat lithium deposition (Fig. 8f–h). Recently, Liu *et al.* found that reduced graphene oxide (r-GO) with initial lithiophilicity exhibited an increasing nucleation overpotential with cycling of the lithium battery.[104] This is mainly because r-

GO possesses catalytic activity that is favorable for the formation of natural SEIs, which impedes the smooth deposition and growth of lithium metal. Therefore, more attention should be paid to avoiding the introduction of catalysts that promote SEI formation when designing lithiophilic host materials for lithium metal anodes.

For most 3D porous electrodes, there is a trade-off between the volumetric capacity and gravimetric capacity. Although the application of 3D hosts favors fast lithium ion transport, promotes sufficient reactions of metallic lithium anodes and improves the gravimetric capacity and cycling stability of lithium batteries, their loose and porous structures lead to low volumetric capacity and cell energy. As a result, some strategies to increase the loading amount and optimize the loading

method of lithium have been developed to densify the 3D porous lithium anodes while keeping the high specific capacity of batteries. For example, Zhang *et al.* increased the lithium plating amount by extending the plating time and the obtained densified lithium anode based on 3D carbon nanofiber hybrids exhibited a high volumetric capacity of 1600 mA h cm^{-3}.[105] Li *et al.* and Liang *et al.* adopted the method of pressing lithium with a punching machine and melting infusion, respectively, to load lithium metal into the 3D hosts compactly.[106,107]

5. Conclusions and perspectives

Among various potential metal anodes, such as potassium, sodium, aluminum, magnesium, zinc, *etc.*, lithium is still considered as the most ideal anode for many high-energy density battery systems, such as lithium–sulfur, lithium–air and next-generation lithium ion batteries. With in-depth understanding of lithium dendrites and SEIs and their formation mechanism, chemical properties, microstructures and morphologies through various characterization techniques, the electrochemical performance parameters of lithium batteries including energy density, rate capability and cycling stability have been significantly improved by various strategies (*e.g.*, electrolyte engineering, current collector modification, and construction of artificial SEIs). However, some critical issues regarding the understanding of lithium anodes *via* characterization techniques and practical lithium batteries still await more efforts. These are summarized as follows:

(1) It has been widely accepted that SEIs greatly affect lithium deposition, but our understanding of SEIs is still limited. For example, SEIs can be formed before and after current loading, and their structures and compositions are different, but the accurate transformation process is unknown. This process may influence dendritic lithium formation, because they happen in tandem after the current is loaded. Therefore, more advanced *operando* characterization techniques should be designed to track this process in working lithium batteries.

(2) The chemical properties of SEIs are always detected by XPS with its advanced depth profile measurement; however, the pre-treatment (*e.g.*, washing and drying the sample) may change or damage the initial SEIs, not reflecting the real condition of SEIs in the batteries. Besides, because of the possible X-ray induced beam damage (*e.g.*, on organic components in particular), the potential influence of the X-ray based characterization methods on SEIs should be evaluated carefully as well.[108,109] Therefore, cryogenic XPS should be developed and combined with cryo-TEM to reveal more accurately the structural and chemical state of SEIs.

(3) AFM is a powerful tool, which has not only been used to characterize electrode interfaces in liquid but also offers a way to obtain site-specific mechanical and resistance information on SEIs.[110,111] However, because AFM imaging typically requires relatively smooth sample surfaces, the electrodes studied by AFM are usually thin films, nanofibers/nanopillars and nanoparticles supported by flat substrates, which differ from the most commonly applied 3D bulk electrodes in real lithium batteries. Therefore, it is desirable for AFM measurements to be adapted

and/or coupled with other characterization techniques to uncover the topological, morphological and chemical changes of 3D electrode materials during the battery working process.

(4) The electrolyte plays a critical role in lithium metal batteries. Generally, an ideal electrolyte should perform the following functions: (1) enable high CE, (2) guarantee good operation under lean electrolyte conditions, (3) ensure high stability and safety at high voltage and (4) allow as low a salt concentration as possible at the same time to limit the cost. However, no electrolyte can simultaneously meet these requirements now. Therefore, future efforts for electrolyte engineering should follow this direction and explore high-performance electrolyte systems to promote the early revival of lithium metal batteries.

Except the safety and cycling stability of the lithium metal anode, other factors (*e.g.*, the electrolyte amount, the lithium thickness, and the depth of discharge) with critical importance for practical applications of lithium batteries also deserve attention from both the academia and industry. Different from the lab-scale coin cells in which the electrolyte dosage is usually omitted, the amount of electrolyte added in the real battery packs directly determines the battery energy density. Therefore, more efforts should be devoted to developing high-performance lithium metal batteries with lean electrolytes. Similarly, excessive lithium is usually utilized in coin cells to compensate for the lithium waste by the formation of SEIs and other side reactions. However, recent studies found that the more lithium used, the more side reactions occur and thus thicker SEIs are generated.[112] Besides, thick lithium leads to large volume variations and severe electrolyte consumption, which limit the battery performance under lean electrolyte conditions. Therefore, optimization of the lithium thickness is also a critical step to realize the practical applications of lithium metal batteries. In the discharge process of lithium batteries, lithium ion alloying/insertion brings about changes in the crystalline structure of electrode materials, some of which take place during deep discharge and are irreversible and therefore cause capacity loss. Hence, the depth of discharge is another important factor closely correlated with the cycling stability of lithium batteries. Specifically, the deeper the depth of discharge, the more irreversible phase transformations take place. Thus, optimizing the depth of discharge to explore the balance between higher energy density induced by full discharge and better cycling stability achieved under partial discharge conditions is pivotal for specialized applications. Nowadays, most of the studies on lithium battery performance are based on miniature coin cells with excess lithium foil and electrolyte, which cannot reflect the real working conditions of high-energy density lithium batteries. Therefore, practical scaled-up pouch cells should be reevaluated.

Conflicts of interest

There are no conflicts to declare.

Acknowledgements

and Technology Graduate University, the OIST Proof of Concept (POC) Program, and the OIST R&D Cluster Research Program.

References

1 B. Liu, J. G. Zhang and W. Xu, Advancing lithium metal batteries, *Joule*, 2018, **2**, 833.

2 J. Qian, W. A. Henderson, W. Xu, P. Bhattacharya, M. Engelhard, O. Borodin and J. G. Zhang, High rate and stable cycling of lithium metal anode, *Nat. Commun.*, 2015, **6**, 6362.

3 M. D. Tikekar, S. Choudhury, Z. Tu and L. A. Archer, Design principles for electrolytes and interfaces for stable lithium-metal batteries, *Nat. Energy*, 2016, **1**, 1.

4 J. Liu, Z. Bao, Y. Cui, E. J. Dufek, J. B. Goodenough, P. Khalifah, Q. Li, B. Y. Liaw, P. Liu, A. Manthiram, Y. S. Meng, V. R. Subramanian, M. F. Toney, V. V. Viswanathan, M. S. Whittingham, J. Xiao, W. Xu, J. Yang, X. Q. Yang and J. G. Zhang, Pathways for practical high-energy long-cycling lithium metal batteries, *Nat. Energy*, 2019, **4**, 180.

5 X. B. Cheng, R. Zhang, C. Z. Zhao, F. Wei, J. G. Zhang and Q. Zhang, A review of solid electrolyte interphases on lithium metal anode, *Adv. Sci.*, 2016, **3**, 1500213.

6 T. Kim, W. T. Song, D. Y. Son, L. K. Ono and Y. B. Qi, Lithium-ion batteries: outlook on present, future, and hybridized technologies, *J. Mater. Chem. A*, 2019, **7**, 2942.

7 X. B. Cheng, R. Zhang, C. Z. Zhao and Q. Zhang, Toward safe lithium metal anode in rechargeable batteries: a review, *Chem. Rev.*, 2017, **117**, 10403.

8 K. Xu, Nonaqueous liquid electrolyte for lithium-based rechargeable batteries, *Chem. Rev.*, 2004, **104**, 4303.

9 J. G. Zhang, W. Xu, J. Xiao, X. Cao and J. Liu, Lithium metal anodes with nonaqueous electrolytes, *Chem. Rev.*, 2020, **120**, 13312.

10 J. Xiao, How lithium dendrites form in liquid batteries, *Science*, 2019, **366**, 426.

11 D. Lin, Y. Liu and Y. Cui, Reviving the lithium metal anode for high-energy batteries, *Nat. Nanotechnol.*, 2017, **12**, 194.

12 Q. Zhou, S. Dong, Z. Lv, G. Xu, L. Huang, Q. Wang, Z. Cui and G. Cui, A temperature-responsive electrolyte endowing superior safety characteristic of lithium metal batteries, *Adv. Energy Mater.*, 2019, **10**, 1903441.

13 J. Zhou, T. Qian, J. Liu, M. Wang, L. Zhang and C. Yan, High-safety all-solid-state lithium-metal battery with high-ionic-conductivity thermoresponsive solid polymer electrolyte, *Nano Lett.*, 2019, **19**, 3066.

14 P. Jaumaux, Q. Liu, D. Zhou, X. Xu, T. Wang, Y. Wang, F. Kang, B. Li and G. Wang, Deep-eutectic-solvent-based self-healing polymer electrolyte for safe and long-life lithium-metal batteries, *Angew. Chem., Int. Ed.*, 2020, **59**, 9134.

15 J. Zhu, P. Li, X. Chen, D. Legut, Y. Fan, R. Zhang, Y. Lu, X. Cheng and Q. Zhang, Rational design of graphitic-inorganic Bi-layer artificial SEI for stable lithium metal anode, *Energy Storage Mater.*, 2019, **16**, 426.

16 K. Thanner, A. Varzi, D. Buchholz, S. J. Sedlmaier and S. Passerini, Artificial solid electrolyte interphases for lithium metal electrodes by wet processing: the role of metal salt concentration and solvent choice, *ACS Appl. Mater. Interfaces*, 2020, **12**, 32851.

17 Z. Yu, D. G. Mackanic, W. Michaels, M. Lee, A. Pei, D. Feng, Q. Zhang, Y. Tsao, C. V. Amanchukwu, X. Yan, H. Wang, S. Chen, K. Liu, J. Kang, J. Qin, Y. Cui and Z. Bao, A dynamic, electrolyte-blocking, and single-ion-conductive network for stable lithium-metal anodes, *Joule*, 2019, **3**, 2761.

18 Z. T. Wondimkun, T. T. Beyene, M. A. Weret, N. A. Sahalie, C. J. Huang, B. Thirumalraj, B. A. Jote, D. Wang, W. N. Su, C. H. Wang, G. Brunklaus, M. Winter and B. J. Hwang, Binder-free ultra-thin graphene oxide as an artificial solid electrolyte interphase for anode-free rechargeable lithium metal batteries, *J. Power Sources*, 2020, **450**, 227589.

19 S. Li, T. Liu, J. Yan, J. Flum, H. Wang, F. Lorandi, Z. Wang, L. Fu, L. Hu, Y. Zhao, R. Yuan, M. Sun, J. F. Whitacre and K. Matyjaszewski, Grafting polymer from oxygen-vacancy-rich nanoparticles to enable protective layers for stable lithium metal anode, *Nano Energy*, 2020, **76**, 105046.

20 S. Ye, L. Wang, F. Liu, P. Shi, H. Wang, X. Wu and Y. Yu, g-C_3N_4 derivative artificial organic/inorganic composite solid electrolyte interphase layer for stable lithium metal anode, *Adv. Energy Mater.*, 2020, **10**, 2002647.

21 D. Kang, S. Sardar, R. Zhang, H. Noam, J. Chen, L. Ma, W. Liang, C. Shi and J. P. Lemmon, *In situ* organic SEI layer for dendrite-free lithium metal anode, *Energy Storage Mater.*, 2020, **27**, 69.

22 B. Wu, J. Lochala, T. Taverne and J. Xiao, The interplay between solid electrolyte interface (SEI) and dendritic lithium growth, *Nano Energy*, 2017, **40**, 34.

23 Y. Gu, W. W. Wang, Y. J. Li, Q. H. Wu, S. Tang, J. W. Yan, M. S. Zheng, D. Y. Wu, C. H. Fan, W. Q. Hu, Z. B. Chen, Y. Fang, Q. H. Zhang, Q. F. Dong and B. W. Mao, Designable ultra-smooth ultra-thin solid-electrolyte interphases of three alkali metal anodes, *Nat. Commun.*, 2018, **9**, 1339.

24 F. Zhao, X. Zhou, W. Deng and Z. Liu, Entrapping lithium deposition in lithiophilic reservoir constructed by vertically aligned ZnO nanosheets for dendrite-free Li metal anodes, *Nano Energy*, 2019, **62**, 55.

25 G. Yasin, M. Arif, T. Mehtab, X. Lu, D. Yu, N. Muhammad, M. T. Nazir and H. Song, Understanding and suppression strategies toward stable Li metal anode for safe lithium batteries, *Energy Storage Mater.*, 2020, **25**, 644.

26 X. Liang, Q. Pang, I. R. Kochetkov, M. S. Sempere, H. Huang, X. Sun and L. F. Nazar, A facile surface chemistry route to a stabilized lithium metal anode, *Nat. Energy*, 2017, **2**, 1.

27 H. Huo, X. Li, Y. Chen, J. Liang, S. Deng, X. Gao, K. Doyle-Davis, R. Li, X. Guo, Y. Shen, C. W. Nan and X. Sun, Bifunctional composite separator with a solid-state-battery strategy for dendrite-free lithium metal batteries, *Energy Storage Mater.*, 2020, **29**, 361.

28 R. Pan, R. Sun, Z. Wang, J. Lindh, K. Edström, M. Strømme and L. Nyholm, Sandwich-structured nano/micro fiber-based separators for lithium metal batteries, *Nano Energy*, 2019, **55**, 316.

29 P. J. Kim and V. G. Pol, High performance lithium metal batteries enabled by surface tailoring of polypropylene separator with a polydopamine/graphene layer, *Adv. Energy Mater.*, 2018, **8**, 1802665.

30 C. Li, S. Liu, C. Shi, G. Liang, Z. Lu, R. Fu and D. Wu, Two-dimensional molecular brush-functionalized porous bilayer composite separators toward ultrastable high-current density lithium metal anodes, *Nat. Commun.*, 2019, **10**, 1363.

31 S. Liu, X. Xia, Z. Yao, J. Wu, L. Zhang, S. Deng, C. Zhou, S. Shen, X. Wang and J. Tu, Straw-brick-like carbon fiber cloth/lithium composite electrode as an advanced lithium metal anode, *Small Methods*, 2018, **2**, 1800035.

32 Z. Yu, H. Wang, X. Kong, W. Huang, Y. Tsao, D. G. Mackanic, K. Wang, X. Wang, W. Huang, S. Choudhury, Y. Zheng, C. V. Amanchukwu, S. T. Hung, Y. Ma, E. G. Lomeli, J. Qin, Y. Cui and Z. Bao, Molecular design for electrolyte solvents enabling energy-dense and long-cycling lithium metal batteries, *Nat. Energy*, 2020, **5**, 526.

33 S. Jurng, Z. L. Brown, J. Kim and B. L. Lucht, Effect of electrolyte on the nanostructure of the solid electrolyte interphase (SEI) and performance of lithium metal anodes, *Energy Environ. Sci.*, 2018, **11**, 2600.

34 Q. Li, B. Quan, W. Li, J. Lu, J. Zheng, X. Yu, J. Li and H. Li, Electro-plating and stripping behavior on lithium metal electrode with ordered three-dimensional structure, *Nano Energy*, 2018, **45**, 463.

35 S. Jiao, X. Ren, R. Cao, M. H. Engelhard, Y. Liu, D. Hu, D. Mei, J. Zheng, W. Zhao, Q. Li, N. Liu, B. D. Adams, C. Ma, J. Liu, J.-G. Zhang and W. Xu, Stable cycling of high-voltage lithium metal batteries in ether electrolytes, *Nat. Energy*, 2018, **3**, 739.

36 I. Yoon, S. Jurng, D. P. Abraham, B. L. Lucht and P. R. Guduru, *In situ* measurement of the plane-strain modulus of the solid electrolyte interphase on lithium-metal anodes in ionic liquid electrolytes, *Nano Lett.*, 2018, **18**, 5752.

37 C. Hou, J. Han, P. Liu, C. Yang, G. Huang, T. Fujita, A. Hirata and M. Chen, *Operando* observations of SEI film evolution by mass-sensitive scanning transmission electron microscopy, *Adv. Energy Mater.*, 2019, **9**, 1902675.

38 J. Z. Lee, T. A. Wynn, M. A. Schroeder, J. Alvarado, X. Wang, K. Xu and Y. S. Meng, Cryogenic focused ion beam characterization of lithium metal anodes, *ACS Energy Lett.*, 2019, **4**, 489.

39 O. Sheng, J. Zheng, Z. Ju, C. Jin, Y. Wang, M. Chen, J. Nai, T. Liu, W. Zhang, Y. Liu and X. Tao, In situ construction of a LiF-enriched interface for stable all-solid-state batteries and its origin revealed by Cryo-TEM, *Adv. Mater.*, 2020, **32**, 2000223.

40 C. Liang, X. Zhang, S. Xia, Z. Wang, J. Wu, B. Yuan, X. Luo, W. Liu, W. Liu and Y. Yu, Unravelling the room-temperature atomic structure and growth kinetics of lithium metal, *Nat. Commun.*, 2020, **11**, 5367.

41 Y. Xu, H. Wu, Y. He, Q. Chen, J. G. Zhang, W. Xu and C. Wang, Atomic to nanoscale origin of vinylene carbonate enhanced cycling stability of lithium metal anode revealed by Cryo-transmission electron microscopy, *Nano Lett.*, 2020, **20**, 418.

42 X. Wang, M. Zhang, J. Alvarado, S. Wang, M. Sina, B. Lu, J. Bouwer, W. Xu, J. Xiao, J. G. Zhang, J. Liu and Y. S. Meng, New insights on the structure of electrochemically deposited lithium metal and its solid electrolyte interphases *via* cryogenic TEM, *Nano Lett.*, 2017, **17**, 7606.

43 W. Huang, H. Wang, D. T. Boyle, Y. Li and Y. Cui, Resolving nanoscopic and mesoscopic heterogeneity of fluorinated species in battery solid-electrolyte interphases by cryogenic electron microscopy, *ACS Energy Lett.*, 2020, **5**, 1128.

44 Y. Li, W. Huang, Y. Li, A. Pei, D. T. Boyle and Y. Cui, Correlating structure and function of battery interphases at atomic resolution using cryoelectron microscopy, *Joule*, 2018, **2**, 2167.

45 C. Fiedler, B. Luerssen, M. Rohnke, J. Sann and J. Janek, XPS and SIMS analysis of solid electrolyte interphases on lithium formed by ether-based electrolytes, *J. Electrochem. Soc.*, 2017, **164**, A3742.

46 C. Hou, J. Han, P. Liu, C. Yang, G. Huang, T. Fujita, A. Hirata and M. Chen, *Operando* observations of SEI film evolution by mass-sensitive scanning transmission electron microscopy, *Adv. Energy Mater.*, 2019, **9**, 1902675.

47 E. Peled, The electrochemical behaviour of alkali and alkaline earth metals in nonaqueous battery systems-the solid electrolyte interphase model, *J. Electrochem. Soc.*, 1979, **126**, 2047.

48 P. Bai, J. Li, F. R. Brushett and M. Z. Bazant, Transition of lithium growth mechanisms in liquid electrolytes, *Energy Environ. Sci.*, 2016, **9**, 3221.

49 H. J. S. Sand, On the concentration at the electrodes in a solution, with special reference to the liberation of hydrogen by electrolysis of a mixture of copper sulphate and sulphuric acid, *Philos. Mag.*, 1901, **1**, 45.

50 Y. Liu, D. Lin, Z. Liang, J. Zhao, K. Yan and Y. Cui, Lithium-coated polymeric matrix as a minimum volume-change and dendrite-free lithium metal anode, *Nat. Commun.*, 2016, **7**, 10992.

51 K. Shen, Z. Wang, Z. Bi, Y. Ying, D. Zhang, C. Jin, G. Hou, H. Cao, L. Wu, G. Zheng, Y. Tang, X. Tao and J. Lu, Magnetic field-suppressed lithium dendrite growth for stable lithium-metal batteries, *Adv. Energy Mater.*, 2019, **9**, 1900260.

52 K. Yan, J. Wang, S. Zhao, D. Zhou, B. Sun, Y. Cui and G. Wang, Temperature-dependent nucleation and growth of dendrite-free lithium metal anodes, *Angew. Chem., Int. Ed.*, 2019, **58**, 11364.

53 L. Li, S. Basu, Y. Wang, Z. Chen, P. Hundekar, B. Wang, J. Shi, Y. Shi, S. Narayanan and N. Koratkar, Self-heating-

induced healing of lithium dendrites, *Science*, 2018, **359**, 1513.

54 C. Fang, J. Li, M. Zhang, Y. Zhang, F. Yang, J. Z. Lee, M. H. Lee, J. Alvarado, M. A. Schroeder, Y. Yang, B. Lu, N. Williams, M. Ceja, L. Yang, M. Cai, J. Gu, K. Xu, X. Wang and Y. S. Meng, Quantifying inactive lithium in lithium metal batteries, *Nature*, 2019, **572**, 511.

55 K. N. Wood, E. Kazyak, A. F. Chadwick, K. H. Chen, J. G. Zhang, K. Thornton and N. P. Dasgupta, Dendrites and pits: untangling the complex behavior of lithium metal anodes through *operando* video microscopy, *ACS Cent. Sci.*, 2016, **2**, 790.

56 Y. S. Cohen, Y. Cohen and D. Aurbach, Micromorphological studies of lithium electrodes in alkyl carbonate solutions using *in situ* atomic force microscopy, *J. Phys. Chem. B*, 2000, **104**, 12282.

57 J. Steiger, D. Kramer and R. Mönig, Mechanisms of dendritic growth investigated by *in situ* light microscopy during electrodeposition and dissolution of lithium, *J. Power Sources*, 2014, **261**, 112.

58 M. J. Zachman, Z. Tu, S. Choudhury, L. A. Archer and L. F. Kourkoutis, Cryo-STEM mapping of solid-liquid interfaces and dendrites in lithium-metal batteries, *Nature*, 2018, **560**, 345.

59 Y. Li, Y. Li, A. Pei, K. Yan, Y. Sun, C. Wu, L. M. Joubert, R. Chin, A. L. Koh, Y. Yu, J. Perrino, B. Butz, S. Chu and Y. Cui, Atomic structure of sensitive battery materials and interfaces revealed by cryo-electron microscopy, *Science*, 2017, **358**, 505.

60 G. Xu, J. Li, C. Wang, X. Du, D. Lu, B. Xie, X. Wang, C. Lu, H. Liu, S. Dong, G. Cui and L. Chen, The formation/decomposition equilibrium of LiH and its contribution on anode failure in practical lithium metal batteries, *Angew. Chem.*, 2021, **133**, 2.

61 Z. Ju, J. Nai, Y. Wang, T. Liu, J. Zheng, H. Yuan, Q. Sheng, C. Jin, W. Zheng, Z. Jin, H. Tian, Y. Liu and X. Yao, Biomacromolecules enabled dendrite-free lithium metal battery and its origin revealed by cryo-electron microscopy, *Nat. Commun.*, 2020, **11**, 488.

62 Y. Xu, H. Wu, Y. He, Q. Chen, J. Zhang, W. Xu and C. Wang, Atomic to nanoscale origin of vinylene carbonate enabled cycling stability of lithium metal anode revealed by cryo-transmission electron microscopy, *Nano Lett.*, 2020, **20**, 418.

63 K. Kanamura, S. Shiraishi and Z. Takehara, Electrochemical deposition of very smooth lithium using nonaqueous electrolytes containing HF, *J. Electrochem. Soc.*, 1996, **143**, 2187.

64 R. Mogi, M. Inaba, S. K. Jeong, Y. Iriyama, T. Abe and Z. Ogumi, Effects of some organic additives on lithium deposition in propylene carbonate, *J. Electrochem. Soc.*, 2002, **149**, A1578.

65 J. Guo, Z. Wen, M. Wu, J. Jin and Y. Liu, Vinylene carbonate–LiNO$_3$: A hybrid additive in carbonic ester electrolytes for SEI modification on Li metal anode, *Electrochem. Commun.*, 2015, **51**, 59.

66 Q. Zhao, Z. Tu, S. Wei, K. Zhang, S. Choudhury, X. Liu and L. A. Archer, Building organic/inorganic hybrid interphases

for fast Interfacial transport in rechargeable metal batteries, *Angew. Chem., Int. Ed.*, 2018, **57**, 992.

67 S. Li, H. Dai, Y. Li, C. Lai, J. Wang, F. Huo and C. Wang, Designing Li-protective layer *via* SOCl$_2$ additive for stabilizing lithium–sulfur battery, *Energy Storage Mater.*, 2019, **18**, 222.

68 Y. Ma, Z. Zhou, C. Li, L. Wang, Y. Wang, X. Cheng, P. Zuo, C. Du, H. Huo, Y. Gao and G. Yin, Enabling reliable lithium metal batteries by a bifunctional anionic electrolyte additive, *Energy Storage Mater.*, 2018, **11**, 197.

69 Y. Zhang, J. Qian, W. Xu, S. M. Russell, X. Chen, E. Nasybulin, P. Bhattacharya, M. H. Engelhard, D. Mei, R. Cao, F. Ding, A. V. Cresce, K. Xu and J. G. Zhang, Dendrite-free lithium deposition with self-aligned nanorod structure, *Nano Lett.*, 2014, **14**, 6889.

70 C. Shen, S. Wang, Y. Jin and W. Q. Han, *In situ* AFM imaging of solid electrolyte interfaces on HOPG with ethylene carbonate and fluoroethylene carbonate-based electrolytes, *ACS Appl. Mater. Interfaces*, 2015, **7**, 25441.

71 K. Edstrom, M. Herstedt and D. Abraham, A new look at the solid electrolyte interphase on graphite anodes in Li-ion batteries, *J. Power Sources*, 2006, **153**, 380.

72 J. Qian, W. Xu, P. Bhattacharya, M. Engelhard, W. A. Henderson, Y. Zhang and J.-G. Zhang, Dendrite-free Li deposition using trace-amounts of water as an electrolyte additive, *Nano Energy*, 2015, **15**, 135.

73 G. Wang, X. Xiong, D. Xie, X. Fu, X. Ma, Y. Li, Y. Liu, Z. Lin, C. Yang and M. Liu, Suppressing dendrite growth by a functional electrolyte additive for robust Li metal anodes, *Energy Storage Mater.*, 2019, **23**, 701.

74 X. Fan, L. Chen, X. Ji, T. Deng, S. Hou, J. Chen, J. Zheng, F. Wang, J. Jiang, K. Xu and C. Wang, Highly fluorinated interphases enable high-voltage Li-metal batteries, *Chem*, 2018, **4**, 174.

75 M. Wang, L. Huai, G. Hu, S. Yang, F. Ren, S. Wang, Z. Zhang, Z. Chen, Z. Peng, C. Shen and D. Wang, Effect of LiFSI concentrations to form thickness- and modulus-controlled SEI layers on lithium metal anodes, *J. Phys. Chem. C*, 2018, **122**, 9825.

76 S. Perez Beltran, X. Cao, J.-G. Zhang and P. B. Balbuena, Localized high concentration electrolytes for high voltage lithium–metal batteries: correlation between the electrolyte composition and its reductive/oxidative stability, *Chem. Mater.*, 2020, **32**, 5973.

77 Y. Yamada, J. Wang, S. Ko, E. Watanabe and A. Yamada, Advances and issues in developing salt-concentrated battery electrolytes, *Nat. Energy*, 2019, **4**, 269.

78 X. Ren, S. Chen, H. Lee, D. Mei, M. H. Engelhard, S. D. Burton, W. Zhao, J. Zheng, Q. Li, M. S. Ding, M. Schroeder, J. Alvarado, K. Xu, Y. S. Meng, J. Liu, J. G. Zhang and W. Xu, Localized high-concentration sulfone electrolytes for high-efficiency lithium-metal batteries, *Chem*, 2018, **4**, 1877.

79 S. Chen, J. Zheng, D. Mei, K. S. Han, M. H. Engelhard, W. Zhao, W. Xu, J. Liu and J. G. Zhang, High-voltage lithium-metal batteries enabled by localized high-concentration electrolytes, *Adv. Mater.*, 2018, **30**, 1706102.

80 L. Yu, S. Chen, H. Lee, L. Zhang, M. H. Engelhard, Q. Li, S. Jiao, J. Liu, W. Xu and J. G. Zhang, A localized high-concentration electrolyte with optimized solvents and lithium difluoro(oxalate)borate additive for stable lithium metal batteries, *ACS Energy Lett.*, 2018, **3**, 2059.

81 W. J. Kwak, H. S. Lim, P. Gao, R. Feng, S. Chae, L. Zhong, J. Read, M. H. Engelhard, W. Xu and J. G. Zhang, Effects of fluorinated diluents in localized high-concentration electrolytes for lithium–oxygen batteries, *Adv. Funct. Mater.*, 2020, 2002927.

82 C. S. Rustomji, Y. Yang, T. K. Kim, J. Mac, Y. J. Kim, E. Caldwell, H. Chung and Y. S. Meng, Liquefied gas electrolytes for electrochemical energy storage devices, *Science*, 2017, **356**, eaal4263.

83 Y. Yang, D. M. Davies, Y. Yin, O. Borodin, J. Z. Lee, C. Fang, M. Olguin, Y. Zhang, E. S. Sablina, X. Wang, C. S. Rustomji and Y. S. Meng, High-efficiency lithium-metal anode enabled by liquefied gas electrolytes, *Joule*, 2019, **3**, 1986.

84 S. Gao, F. Sun, N. Liu, H. Yang and P.-F. Cao, Ionic conductive polymers as artificial solid electrolyte interphase films in Li metal batteries-a review, *Mater. Today*, 2020, **40**, 140.

85 E. Kazyak, K. N. Wood and N. P. Dasgupta, Improved cycle life and stability of lithium metal anodes through ultrathin atomic layer deposition surface treatments, *Chem. Mater.*, 2015, **27**, 6457.

86 N. J. Dudney, Addition of a thin-film inorganic solid electrolyte (LiPON) as a protective film in lithium batteries with a liquid electrolyte, *J. Power Sources*, 2000, **89**, 176.

87 N. W. Li, Y. X. Yin, C. P. Yang and Y. G. Guo, An artificial solid electrolyte interphase layer for stable lithium metal anodes, *Adv. Mater.*, 2016, **28**, 1853.

88 J. Zhao, L. Liao, F. Shi, T. Lei, G. Chen, A. Pei, J. Sun, K. Yan, G. Zhou, J. Xie, C. Liu, Y. Li, Z. Liang, Z. Bao and Y. Cui, Surface fluorination of reactive battery anode materials for enhanced stability, *J. Am. Chem. Soc.*, 2017, **139**, 11550.

89 G. Zheng, C. Wang, A. Pei, J. Lopez, F. Shi, Z. Chen, A. D. Sendek, H.-W. Lee, Z. Lu, H. Schneider, M. M. Safont-Sempere, S. Chu, Z. Bao and Y. Cui, High-performance lithium metal negative electrode with a soft and flowable polymer coating, *ACS Energy Lett.*, 2016, **1**, 1247.

90 Y. Gao, Z. Yan, J. L. Gray, X. He, D. Wang, T. Chen, Q. Huang, Y. C. Li, H. Wang, S. H. Kim, T. E. Mallouk and D. Wang, Polymer–inorganic solid-electrolyte interphase for stable lithium metal batteries under lean electrolyte conditions, *Nat. Mater.*, 2019, **18**, 384.

91 S. Liu, X. Xia, S. Deng, D. Xie, Z. Yao, L. Zhang, S. Zhang, X. Wang and J. Tu, In situ solid electrolyte interphase from spray quenching on molten Li: a new way to construct high-performance lithium-metal anodes, *Adv. Mater.*, 2019, **31**, 1806470.

92 N. W. Li, Y. Shi, Y. X. Yin, X. X. Zeng, J. Y. Li, C. J. Li, L. J. Wan, R. Wen and Y. G. Guo, A flexible solid electrolyte interphase layer for long-life lithium metal anodes, *Angew. Chem., Int. Ed.*, 2018, **57**, 1505.

93 B. Han, D. Feng, S. Li, Z. Zhang, Y. Zou, M. Gu, H. Meng, C. Wang, K. Xu, Y. Zhao, H. Zeng, C. Wang and Y. Deng, Self-regulated phenomenon of inorganic artificial solid electrolyte interphase for lithium metal batteries, *Nano Lett.*, 2020, **20**, 4029.

94 S. Jin, Y. Jiang, H. Ji and Y. Yu, Advanced 3D current collectors for lithium-based batteries, *Adv. Mater.*, 2018, **30**, 1802014.

95 S. Ni, S. Tan, Q. An and L. Mai, Three dimensional porous frameworks for lithium dendrite suppression, *J. Energy Chem.*, 2020, **44**, 73.

96 S. Liu, X. Xia, Y. Zhong, S. Deng, Z. Yao, L. Zhang, X.-B. Cheng, X. Wang, Q. Zhang and J. Tu, 3D TiC/C core/shell nanowire skeleton for dendrite-free and long-life lithium metal anode, *Adv. Energy Mater.*, 2018, **8**, 1702322.

97 S.-S. Chi, Y. Liu, W.-L. Song, L.-Z. Fan and Q. Zhang, Prestoring lithium into stable 3D nickel foam host as dendrite-free lithium metal anode, *Adv. Funct. Mater.*, 2017, **27**, 1700348.

98 H. Zhao, D. Lei, Y.-B. He, Y. Yuan, Q. Yun, B. Ni, W. Lv, B. Li, Q.-H. Yang, F. Kang and J. Lu, Compact 3D copper with uniform porous structure derived by electrochemical dealloying as dendrite-free lithium metal anode current collector, *Adv. Energy Mater.*, 2018, **8**, 1800266.

99 Z. Sun, S. Jin, H. Jin, Z. Du, Y. Zhu, A. Cao, H. Ji and L. J. Wan, Robust expandable carbon nanotube scaffold for ultrahigh-capacity lithium-metal anodes, *Adv. Mater.*, 2018, **30**, 1800884.

100 G. Yang, Y. Li, Y. Tong, J. Qiu, S. Liu, S. Zhang, Z. Guan, B. Xu, Z. Wang and L. Chen, Lithium plating and stripping on carbon nanotube sponge, *Nano Lett.*, 2019, **19**, 494.

101 W. Liu, P. Liu and D. Mitlin, Tutorial review on structure-dendrite growth relations in metal battery anode supports, *Chem. Soc. Rev.*, 2020, **49**, 7284.

102 G. Huang, J. Han, F. Zhang, Z. Wang, H. Kashani, K. Watanabe and M. Chen, Lithiophilic 3D nanoporous nitrogen-doped graphene for dendrite-free and ultrahigh-rate lithium-metal anodes, *Adv. Mater.*, 2019, **31**, 1805334.

103 P. Zhai, Y. Wei, J. Xiao, W. Liu, J. Zuo, X. Gu, W. Yang, S. Cui, B. Li, S. Yang and Y. Gong, In situ generation of artificial solid-electrolyte interphases on 3D conducting scaffolds for high-performance lithium-metal anodes, *Adv. Energy Mater.*, 2020, **10**, 1903339.

104 W. Liu, Y. Xia, W. Wang, Y. Wang, J. Jin, Y. Chen, E. Paek and D. Miltin, Pristine or highly defective? Understanding the role of graphene structure for stable lithium metal plating, *Adv. Energy Mater.*, 2019, **9**, 1802918.

105 C. Zhang, S. Liu, G. Li, C. Zhang, X. Liu and J. Luo, Incorporating ionic paths into 3D conducting scaffolds for high volumetric and areal capacity, high rate lithium-metal anodes, *Adv. Mater.*, 2018, **30**, 1801328.

106 Q. Li, S. Zhu and Y. Lu, 3D porous Cu current collector/Li-metal composite anode for stable lithium-metal batteries, *Adv. Funct. Mater.*, 2017, **27**, 1606422.

107 Z. Liang, D. Lin, J. Zhao, Z. Lu, Y. Liu, C. Liu, Y. Lu, H. Wang, K. Yan, X. Tao and Y. Cui, Composite lithium

metal anode by melt infusion of lithium into a 3D conducting scaffold with lithiophilic coating, *Proc. Natl. Acad. Sci. U. S. A.*, 2016, **113**, 2862.

108 A. Neuhold, J. Novak, H. Flesch, A. Moser, T. Djuric, L. Grodd, S. Grigorian, U. Pietsch and R. Resel, X-ray radiation damage of organic semiconductor thin films during grazing incidence diffraction experiments, *Nucl. Instrum. Methods Phys. Res., Sect. B*, 2012, **284**, 64.

109 P. Laibinis, R. Graham, H. Biebuyck and G. Whitesides, X-ray damage to CFCO-terminated organic monolayers on Si/Au: principal effect of electrons, *Science*, 1991, **254**, 983.

110 M. Lee, R. Reddi, J. Choi, J. Liu, X. Huang, H. Cho and J. Kim, In-*operando* AFM characterization of mechanical property evolution of Si anode binders in liquid electrolyte, *ACS Appl. Energy Mater.*, 2020, **3**, 1899.

111 W. Liu, P. Liu and D. Mitlin, Review of emerging concepts in SEI analysis and artificial SEI membranes for lithium, sodium, and potassium metal battery anodes, *Adv. Energy Mater.*, 2020, **10**, 2002297.

112 C. Niu, D. Liu, J. Lochala, C. Anderson, X. Cao, M. Gross, W. Xu, J. Zhang, M. Whittingham, J. Xiao and J. Liu, Balancing interfacial reactions to achieve long cycle life in high-energy lithium metal batteries, *Nat. Energy*, 2021, **6**, 723.